



This is a repository copy of *Direct evidence of ultrafast energy delocalization between optically hybridized J-aggregates in a strongly coupled microcavity*.

White Rose Research Online URL for this paper:

<https://eprints.whiterose.ac.uk/217347/>

Version: Accepted Version

---

**Article:**

Russo, M., Georgiou, K., Genco, A. et al. (6 more authors) (2024) Direct evidence of ultrafast energy delocalization between optically hybridized J-aggregates in a strongly coupled microcavity. *Advanced Optical Materials*, 12 (25). 2400821. ISSN 2195-1071

<https://doi.org/10.1002/adom.202400821>

---

© 2024 The Authors. Except as otherwise noted, this author-accepted version of a journal article published in *Advanced Optical Materials* is made available via the University of Sheffield Research Publications and Copyright Policy under the terms of the Creative Commons Attribution 4.0 International License (CC-BY 4.0), which permits unrestricted use, distribution and reproduction in any medium, provided the original work is properly cited. To view a copy of this licence, visit <http://creativecommons.org/licenses/by/4.0/>

**Reuse**

This article is distributed under the terms of the Creative Commons Attribution (CC BY) licence. This licence allows you to distribute, remix, tweak, and build upon the work, even commercially, as long as you credit the authors for the original work. More information and the full terms of the licence here:

<https://creativecommons.org/licenses/>

**Takedown**

If you consider content in White Rose Research Online to be in breach of UK law, please notify us by emailing [eprints@whiterose.ac.uk](mailto:eprints@whiterose.ac.uk) including the URL of the record and the reason for the withdrawal request.



[eprints@whiterose.ac.uk](mailto:eprints@whiterose.ac.uk)  
<https://eprints.whiterose.ac.uk/>

1 **Direct Evidence of Ultrafast Energy Delocalization Between Optically Hybridized J-**  
2 **Aggregates in a Strongly Coupled Microcavity**

3  
4 *Mattia Russo, Kyriacos Georgiou, Armando Genco, Simone De Liberato, Giulio Cerullo,*  
5 *David G. Lidzey, Andreas Othonos, Margherita Maiuri\*, Tersilla Virgili\**

6  
7 M. Russo, A. Genco, G. Cerullo, M. Maiuri

8 Dipartimento di Fisica, Politecnico di Milano, Piazza Leonardo da Vinci 32, Milano Italy.

9 E-mail: margherita.maiuri@polimi.it

10  
11 M. Russo, S. De Liberato, G. Cerullo, T. Virgili

12 Istituto di Fotonica e Nanotecnologie – Consiglio Nazionale delle Ricerche (CNR), Piazza

13 Leonardo da Vinci 32, Milano Italy

14 E-mail: tersilla.virgili@cnr.it

15  
16 K. Georgiou, A. Othonos

17 Department of Physics, Laboratory of Ultrafast Science, University of Cyprus, P.O. Box

18 20537, Nicosia 1678, Cyprus

19  
20 D. G. Lidzey

21 Department of Physics and Astronomy, University of Sheffield, Hicks Building, Hounsfield

22 Road, Sheffield S3 7RH, UK

23  
24 S. De Liberato

25 School of Physics and Astronomy, University of Southampton, Southampton SO17 1BJ, UK

26  
27  
28  
29  
30 **Keywords:** Strong coupling, Energy delocalization, 2D Spectroscopy, Polariton states,  
31 organic microcavities

## 1 ABSTRACT

2 Strong coupling between light and matter in a microcavity can produce quasi-particle states  
3 termed cavity-polaritons. In cavity architectures containing more than one excitonic species,  
4 the photon mode can simultaneously couple to the different excitons, generating new ‘hybrid-  
5 polariton’ states. It has been demonstrated that such hybrid polariton states can energetically  
6 connect different molecular species, even when their intermolecular distance is much larger  
7 than the Förster transfer radius. Here, we unveil this mechanism and observe in the time domain  
8 energy delocalization in a strongly coupled cavity containing two layers of donor and acceptor  
9 molecules, separated by an inert spacer layer of 2  $\mu\text{m}$  thickness. We use two-dimensional  
10 electronic spectroscopy, a technique that provides simultaneously high spectral and temporal  
11 resolution, to probe the dynamics of the energy flow processes following ultra-fast excitation.  
12 We show that energy is almost instantaneously delocalized among the polariton states,  
13 providing a direct connection between very highly separated donor and acceptor molecules.  
14 Our results are of potential significance for light-harvesting devices, optoelectronics and bio-  
15 photonic systems.

16

17 **1. Introduction**

18 Optically active materials placed inside microcavities can experience enhanced light-matter  
19 interactions and, under certain conditions, form hybrid quasiparticles called polaritons<sup>1</sup>. In the  
20 so-called strong coupling regime, light and matter reversibly exchange energy, with the newly  
21 formed polariton states being described by a linear quantum superposition of cavity photons  
22 and matter excitations<sup>2</sup>. Owing to their unique properties and the wealth of phenomena they can  
23 induce, polaritons have long been of great interest<sup>3-7</sup>. Organic-polaritons are characterized by  
24 an enhanced stability at room temperature, stemming from the high binding energy of Frenkel  
25 excitons in organic semiconducting materials<sup>8,9</sup>. Therefore, they have been used as testbeds for  
26 studies of fundamental physics without the necessity of cooling to cryogenic temperatures<sup>10-13</sup>.  
27 Recent experimental and theoretical studies have shown that, apart from non-linear polariton  
28 many-body phenomena observed under intense excitation conditions<sup>14-19</sup>, the photophysical  
29 functionalities of organic materials could potentially<sup>20,21</sup> be altered through their hybridization  
30 with cavity photons in the low-excitation regime<sup>22-26</sup>, or even in the complete absence of optical  
31 excitation<sup>27-29</sup>.

32 By strongly coupling more than one excitonic resonance to the same confined photonic  
33 mode, new eigenstates emerge that are formally described as a mixture of the photon and of the  
34 different excitons. If the different excitons are located in distant materials inside the microcavity,

1 the polaritonic coupling allows long-range energy transfer (ET) between spatially separated  
2 donor-acceptor molecular aggregates that are hybridized through their mutual coupling to the  
3 same optical mode<sup>30-33</sup>. Importantly, unlike other nonradiative dipole-dipole ET mechanisms,  
4 polariton-mediated energy transfer is not limited by the separation between donor and acceptor  
5 molecular species. Rather, the large exciton oscillator strengths permit a coupling between  
6 molecules having different electronic energy transitions<sup>33</sup> over mesoscopic distances of several  
7 microns<sup>34</sup>. We note that other physical properties – such as cavity photon lifetime and exciton  
8 broadening – also affect the hybridization of the excitonic states and can modify ET processes.

9 Theoretical work by Sánchez Muñoz and coworkers<sup>35</sup> has demonstrated that the  
10 temporal evolution of the energy flow in such coupled systems depends on the degree of  
11 hybridization between the various polariton states. Indeed, narrow, and spectrally well-  
12 separated excitonic transitions lead to polariton states having a greater degree of hybridization,  
13 with the excitonic contribution being (in some cases) comparable to that of the cavity photon.  
14 This results in polaritons having a wavefunction that is spatially delocalized throughout the  
15 entire microcavity, enabling an ultrafast energy redistribution among polariton-states.

16 Ultrafast spectroscopy is a powerful tool to probe carrier dynamics and energy transfer  
17 processes in materials and devices<sup>33,36-43</sup>. However, when applied to study polariton relaxation  
18 dynamics, ultrafast experiments become very challenging to perform and to interpret<sup>44</sup> due to  
19 two factors: (i) the ultrashort lifetime of the cavity photons, typically of the order of few tens  
20 of femtoseconds, depending on the cavity Q factor, and (ii) the ultrafast polariton decay, mainly  
21 dominated by relaxation towards dark states. These are formalized by the Tavis-Cummings  
22 model<sup>45</sup> and are also understood as resulting from uncoupled excitons that exist in a ‘reservoir’  
23 of states<sup>26,46-48</sup>.

24 To probe timescales on which polaritons are coherent (i.e. when the wavefunctions of  
25 excitons and photons are inseparably mixed<sup>26,36,44</sup>), it is necessary to use ultra-short laser pulses  
26 whose duration is shorter than the lifetime of polaritons. Two-dimensional electronic  
27 spectroscopy (2DES)<sup>49,50</sup> is a powerful technique which allows one to achieve high temporal  
28 resolution while, at the same time, providing high spectral resolution over the excitation  
29 frequency. Three delayed laser pulses are used in 2DES, with the excitation energy axis being  
30 obtained by performing a Fourier transform of the signal with respect to the coherence time  $t_1$   
31 between the first two pump pulses. The temporal evolution of the system is then obtained by  
32 scanning the delay  $t_2$  (waiting time) between the second and the third pulse, the latter acting as  
33 a probe.

1 Recently 2DES has been applied to study ultrafast dynamics in a few microcavity  
2 structures<sup>51,52,53</sup>. Notably, Son and coworkers<sup>53</sup> evidenced an energy cascade process in donor-  
3 acceptor cavities containing films of semiconducting carbon nanotubes distanced by about 150  
4 nm, with a transfer from the highest- to the lowest-energy polariton state occurring in 200 fs.  
5 However, in the limit of narrow excitonic transitions and significant photonic components of  
6 the polariton states, they predicted the upper-to-lower energy relaxation to become quasi-  
7 instantaneous. This was not observed due to the largely excitonic nature of the polaritons  
8 formed in the cavities studied. Therefore, forming highly hybridized polaritons and showing  
9 experimentally the inherent instantaneous energy redistribution over mesoscopic distances,  
10 remains a challenge.

11 In this work, we report the fabrication of a microcavity containing two thin films of J-  
12 aggregated organic semiconductors (named TDBC and NK2707), where the J-aggregate layers  
13 are separated by a micron-thick, inert and transparent spacer. Here, strong coupling to the cavity  
14 photon-mode results in the formation of a series of hybrid-polariton states. In this system,  
15 excitonic transitions are sufficiently narrow and spectrally separated, leading to hybridized  
16 polariton states containing a significant photon component, as well as a mixture of the two  
17 excitons.

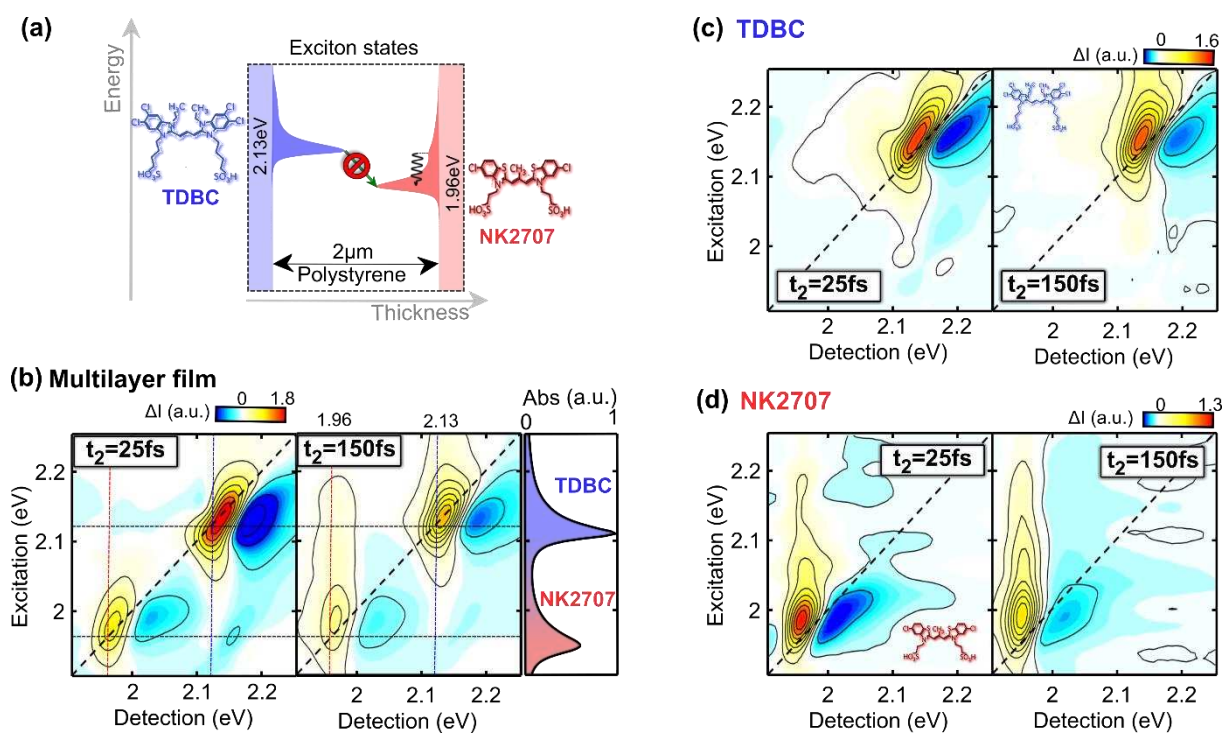
18 We use 2DES to characterize the energy flow mechanisms between the polariton states  
19 both temporally and spectrally. Our measurements provide direct evidence of ultrafast  
20 mesoscopic energy delocalization and coupling between the molecules in the different layers  
21 driven by polariton hybridization. Our results agree with theoretical predictions for systems in  
22 which polariton states have strong photon character. Our findings have relevance for the  
23 development of advanced optoelectronic devices exploiting polaritons to enhance energy  
24 transfer, and for the understanding of energy-harvesting processes in bio-photonic architectures  
25 <sup>54,55</sup>.

26

## 27 **2. Results**

28 As the active materials in our experiments, we have used the molecular dyes 5,6  
29 dichloro-2-[[5,6-dichloro-1-ethyl-3-(4-sulphobutyl)- benzimidazol-2-ylidene]-propenyl]-1-  
30 ethyl-3-(4-sulphobutyl)-benzimidazolium hydroxide, sodium salt, inner salt (TDBC) and 5-  
31 chloro-2-[3-[5-chloro-3-(3-sulphopropyl)- 2(3H)-benzothiazolylidene]-2-methyl-1-propenyl]-  
32 3-(3-sulphopropyl)- benzothiazolium hydroxide, inner salt, compound with triethylamine  
33 (NK2707). These were dispersed into a transparent polymeric matrix (gelatine) and cast into

1 thin films by spin-coating. Upon aggregation, such dyes form J-aggregates which result from  
 2 phase-separation and subsequent crystallization / self-assembly of the cyanine dyes placed in a  
 3 matrix<sup>31</sup>. In these aggregates electronic coupling between molecular dipoles creates  
 4 delocalized, red-shifted and spectrally narrowed excitonic states. We have used a sequential  
 5 spin-coating technique to create a multilayer structure in which J-aggregated TDBC and  
 6 NK2707 dye layers were physically separated from one another using a 2 $\mu\text{m}$  optically  
 7 transparent polystyrene (PS) spacer layer. The mesoscopic thickness of the PS spacer layer,  
 8 which is much larger than the Förster radius, prevents direct ET between the J-aggregated dyes.  
 9 Figure 1a shows a schematic of the multilayer film, together with the chemical structure and  
 10 the steady state absorption of both J-aggregated dyes. The TDBC J-aggregate (highlighted in  
 11 blue) has an absorption peak at 2.13eV, while the absorption of the NK2707 aggregate (plotted  
 12 in red) peaks at lower energy (1.96eV) together with a broad shoulder that peaks around 2.13eV.  
 13



14  
 15 **Figure 1.** (a) Schematic representation of the multilayer film accompanied by the steady state  
 16 absorption and molecular structure of the NK2707 (red) and TDBC (blue). Here the black wavy  
 17 arrow corresponds to an intramolecular energy relaxation process in NK2707. (b) Steady state  
 18 absorption spectrum (right) of the non-cavity control film and purely absorptive 2DES maps at  
 19  $t_2 = 25\text{fs}$  (left) and  $150\text{fs}$  (middle), where the spectral positions of the TDBC and NK2707  
 20 exciton states are identified using horizontal and vertical dashed lines. (c) Purely absorptive

1 2DES maps of a TDBC single film at  $t_2 = 25$ fs (left) and 150fs (right). (d) Purely absorptive  
2 2DES maps of a NK2707 single film at  $t_2 = 25$ fs (left) and 150fs (right).

3

4 We first use broadband 2DES to demonstrate the absence of direct ET between the two  
5 J-aggregated dyes in the multilayer film. Broadband laser pulses, spanning from 1.88 eV to 2.25  
6 eV, temporally compressed to 15 fs, were used to pump and probe the excitonic population of  
7 the two J-aggregates. The 2DES apparatus is described in the Methods section. Figure 1b shows  
8 2DES maps of the multilayer recorded at waiting times  $t_2 = 25$  fs and 150 fs, together with  
9 steady state absorption spectrum in the right panel.

10 At  $t_2 = 25$  fs, the 2DES map is composed of two diagonal signals in correspondence with  
11 the absorption peaks of the two species, with no cross peaks being evident. Each of these signals  
12 contains a positive peak, corresponding to the ground state bleaching (GSB) and stimulated  
13 emission (SE) of the excitonic transition, and a negative peak at slightly higher photon energies,  
14 corresponding to a photoinduced absorption (PA) due to the transition from exciton states to  
15 energetically higher excited states<sup>56,57</sup>. At  $t_2 = 150$  fs, we observe the formation of a positive  
16 cross peak that corresponds to excitation over the spectral range covering 2eV to 2.2eV and  
17 detection at 1.96eV (the absorption peak of NK2707). This peak could either represent direct  
18 ET from TDBC (the donor) to NK2707 (the acceptor) or a simple internal relaxation process  
19 within NK2707, in which excitons scatter from higher to lower energy states. To determine the  
20 nature of this process, 2DES was performed on films of pure TDBC and NK2707 with the same  
21 thickness and concentration as used in the multilayer film.

22 Figure 1c shows the 2DES maps of a TDBC thin film at  $t_2 = 25$  fs and 150 fs. At both  
23 time delays, a diagonal peak reflecting the steady-state absorption is observed. The main  
24 difference between the two 2DES maps relates to the lineshape of the diagonal peaks;  
25 specifically, the peak observed at  $t_2 = 25$  fs has an elliptical shape and is stretched along the  
26 diagonal. At  $t_2 = 150$  fs this feature has broadened along the anti-diagonal direction. This  
27 process is typical in molecular materials, and results from spectral diffusion effects and loss of  
28 excitation memory<sup>58</sup>.

29 Figure 1d shows 2DES maps of a NK2707 film at  $t_2 = 25$  fs and 150 fs. Here the maps  
30 are dominated by an intense absorption peak at 1.96eV that is located along the diagonal line.  
31 We observe the build-up of a cross peak at 1.96eV following excitation in the spectral range  
32 2eV to 2.2 eV. We attribute such peaks to an internal conversion process from a higher to a  
33 lower energy state at 1.96eV. Such signals are comparable in magnitude with the cross peaks  
34 observed in the multilayer film, implying that there is no direct ET process between the donor

(TDBC) and the acceptor (NK2707) species. Rather, the cross peaks observed in the multilayer films result from an internal conversion mechanism within the NK2707 (see wavy black arrow in Figure 1a). The dynamics of these cross peaks are compared in Figure S1, and no difference is observed between the multilayer film and the film containing NK2707 alone.

We now discuss the ultrafast optical response of the multilayer film when its components are strongly coupled to the optical microcavity. The linear optical properties of this structure have previously been discussed in detail by Georgiou et al.<sup>34</sup>, and it has been demonstrated that the excitonic states of both TDBC and NK2707 are simultaneously strongly coupled to a series of cavity modes<sup>34</sup>. As a result of this coupling, several polariton branches are observed that undergo simultaneous anti-crossing.

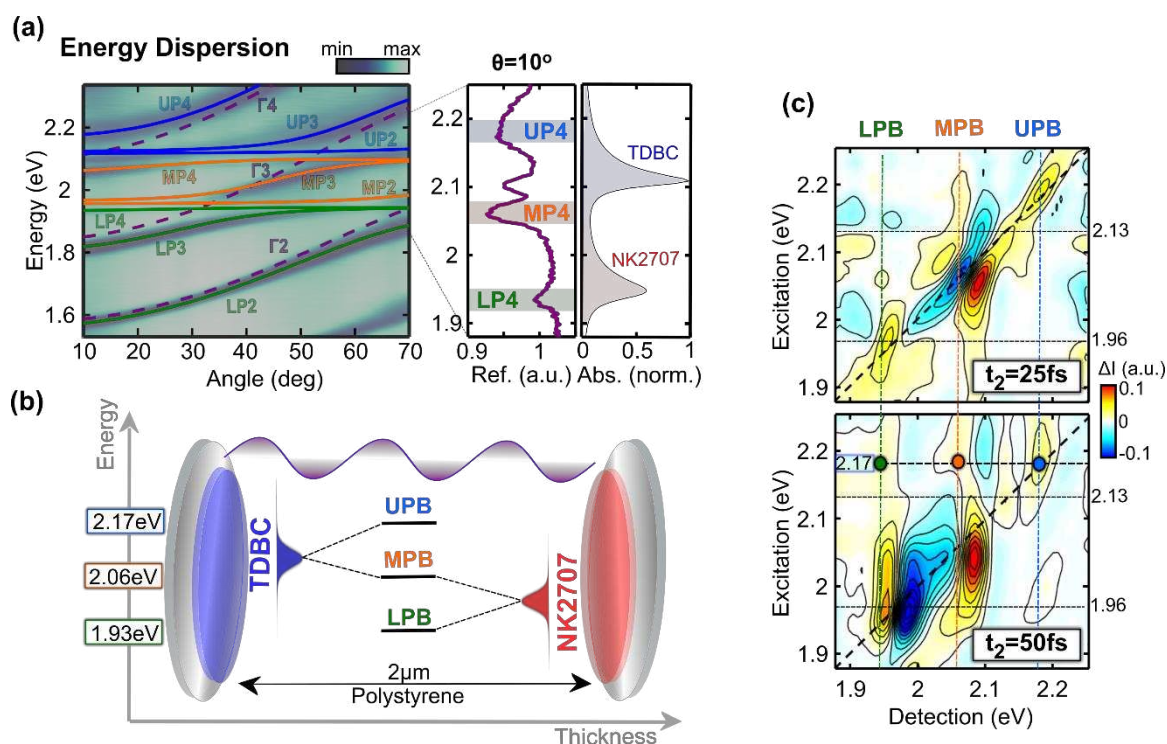


**Figure 2.** (a) Energy dispersion map of the microcavity where the coloured lines indicate the Upper (blue), Middle (orange) and Lower (green) polariton branches calculated using a coupled oscillator model. We also identify the TDBC and NK2707 exciton states and the cavity modes (violet dashed lines). On the right side, there is a zoom in of the reflectivity map at  $10^\circ$  from 1.88eV to 2.25 eV along the energy axis, which corresponds to the region probed in the 2DES experiment. (b) Energy level scheme of the organic microcavity in the strong coupling regime where the energy axis is labelled with the energies of the polariton states; UPB at 2.17eV, MPB at 2.06eV and LPB at 1.93eV. The black dashed lines mark the dominant excitonic contributions to each polariton state. (c) Purely absorptive 2DES spectra at  $t_2 = 25\text{fs}$  (top) and



1 50fs (bottom). The dashed lines along the detection axis represent the position of the polariton  
2 states and the dashed lines along the excitation axis correspond to the excitonic states of  
3 NK2707 (1.96eV) and TDBC (2.13eV).

4  
5 Figure 2a shows angle-dependent white-light optical reflectivity measurements of the  
6 cavity to map out the dispersion of the polariton branches over an angular range between 10°  
7 and 70°, as previously measured<sup>34</sup>. Due to the substantial thickness of the cavity spacer layer  
8 (leading to a significant optical cavity path-length), multiple cavity modes are supported  
9 (labelled  $\Gamma 2$ ,  $\Gamma 3$  and  $\Gamma 4$ ), each of which undergoes anticrossing when they come into resonance  
10 with the two molecular species (see absorption spectra shown in the right side of the panel).  
11 This ladder of cavity modes results in a series of different polariton modes that we term as  
12 upper, middle and lower polaritons (UP, MP, LP). We describe the energy dispersion of these  
13 polariton modes using an n-level coupled-oscillator model fit as shown in Figure 2a, with  
14 relevant parameters and Hopfield coefficients reported in Supporting Information (Table S1  
15 and Figure S2). The exact photon/exciton character of the different polariton branches is  
16 dependent on energetic detuning and angle of observation, however it has been previously  
17 shown that for the upper UP and LP the cavity mode is preferentially mixed with a substantial  
18 fraction of either TDBC or NK2707, respectively<sup>34</sup>. In contrast, the MP contains an admixture  
19 of the cavity mode with both molecular species<sup>34</sup>.

20 Here, we focus on the polariton states covered by the spectrum of our laser (from 1.88eV  
21 to 2.25eV) and measurement angle (10°), highlighted in the zoom out of Figure 2a, right panel.  
22 It is apparent that there are several polariton states within the measurement window (namely  
23 LP4, MP4 and UP3,4). In what follows, we focus our discussion by describing the series of  
24 polariton states coupled with photon-mode  $\Gamma 4$ . For simplicity, we refer to UP4 (at 2.17 eV) as  
25 UPB, MP4 (at 2.06 eV) as MPB and LP4 (at 1.93 eV) at the LPB as sketched in Figure 2b. The  
26 rationale to exclude UP3 from our analysis is that in multimode polariton systems, photonic  
27 modes exist in a ‘decoupled’ regime which has been theoretically predicted<sup>59,60</sup> and  
28 experimentally observed<sup>61,62</sup>. Thus in our cavity, the various photonic modes are not coupled to  
29 each other and the sets of polariton-states generated (LP, UP and MP) can be treated  
30 individually.

31 Figure 2c shows the 2DES maps obtained for the organic microcavity for 10° incidence  
32 angle at  $t_2 = 25$  fs and 50 fs. In this experiment, we pump the cavity using broadband laser  
33 pulses and record its transient reflectivity ( $\Delta R$ ). Here, the main polariton contributions to the  
34 probe signal are identified via different coloured areas (LPB – green, MP B– orange, UPB –

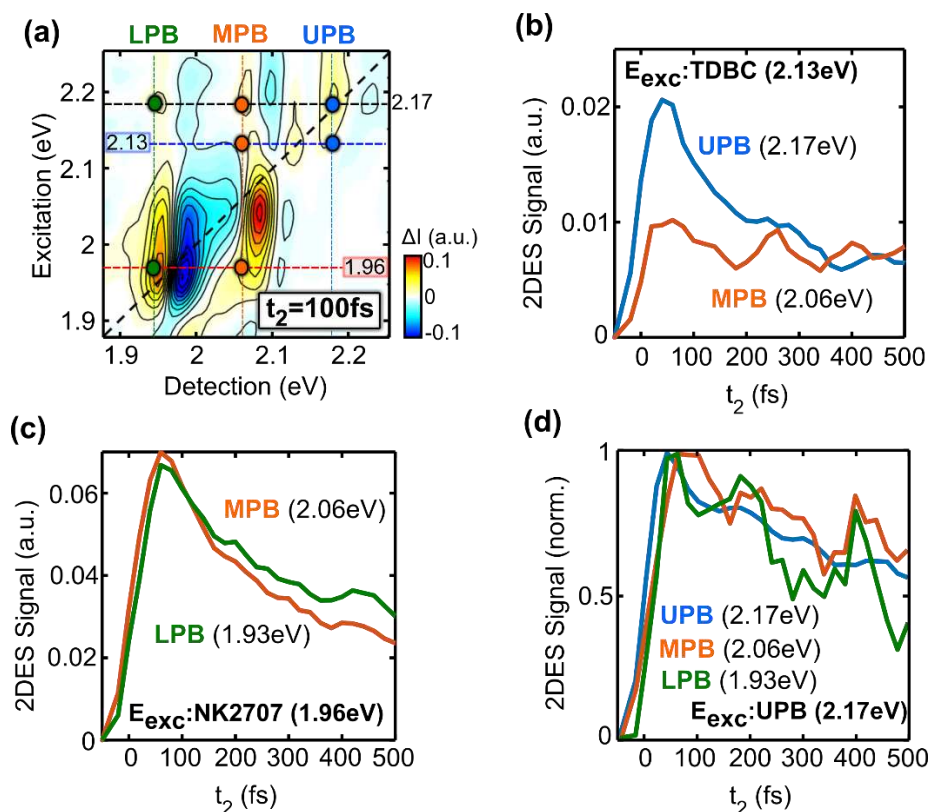
1 blue). We identify the energies of the different polariton states via vertical lines in the 2DES  
2 maps, with the energy of the uncoupled excitons shown using horizontal lines.

3 At  $t_2 = 25$  fs we observe three diagonal peaks that correspond to transient signals of each  
4 polariton state. These peaks have a derivative lineshape with contributions from both negative  
5 and positive signals. This effect results from the fact that when an organic exciton-polariton is  
6 pumped, the refractive index of the active material and the oscillator strength of the exciton  
7 peak are reduced<sup>17, 63</sup>. This causes a contraction of the Rabi splitting and a near instantaneous  
8 blue/red-shift of the polariton states, resulting in a derivative lineshape of the 2DES signal. At  
9  $t_2 = 50$  fs we find that the 2DES map includes cross peaks detected at MPB and LPB energies  
10 as a result of excitation of the UPB state, marked in the 2DES map with orange (MPB) and  
11 green (LPB) circles. Such signals are a signature of a transfer mechanism between the polariton  
12 states and, consequently, between the TDBC and NK2707 molecules.

13

### 14 **3. Discussion**

15 In this section, we investigate possible energy transfer pathways between the donor and  
16 acceptor dyes assisted by the polariton states via an analysis of the dynamics of the cross peaks,  
17 which represent transient absorption signal of the system detected at an energy that is different  
18 with respect to the excitation energy. Figure 3a shows a 2DES map of the organic microcavity  
19 at  $t_2 = 100$  fs; here the horizontal dashed lines correspond to excitation of the following states:  
20 UPB (2.17 eV), TDBC exciton (2.13 eV) and NK2707 exciton (1.96 eV). Figures 3b, c and d  
21 plot the measured dynamics of the cross peaks identified in panel (a) as a function of the waiting  
22 time  $t_2$ .



1  
2 **Figure 3.** 2DES time traces: (a) Purely absorptive 2D map at  $t_2 = 100\text{fs}$  used to highlight specific  
3 dynamics at selected excitation/detection energies. (b)  $t_2$  traces obtained by exciting the TDBC  
4 exciton (2.13eV) and detecting the UPB (2.17eV, blue) and MPB (2.06eV, orange) states. (c)  
5  $t_2$  traces obtained by exciting the NK2707 exciton (1.96eV) and detecting the MPB (2.06eV,  
6 orange) and LPB (1.93eV, green) states. (d) normalized  $t_2$  traces obtained by exciting the UPB  
7 (2.17eV) and detecting the UPB (2.17eV blue), MPB (2.06eV, orange) and LPB (1.93eV,  
8 green) states. The dynamics reported in panels (b), (c) and (d) correspond to the points in the  
9 2D map of panel (a) that are emphasized with dashed lines and coloured circles.

10  
11 We first focus on the polariton cross peaks that result from the excitation of the  
12 uncoupled exciton reservoir. This is shown in Figure 3b where we plot dynamics obtained by  
13 excitation at 2.13eV (corresponding to the TDBC exciton) and detection of the cross peaks at  
14 2.06eV (MPB, orange) and 2.17eV (UPB, blue). Both dynamics have a rise time comparable  
15 with the  $\approx 20\text{fs}$  temporal resolution of the experiment. This suggests that once the TDBC  
16 reservoir excitons have been created, an immediate coherent coupling to the cavity occurs,  
17 resulting in instantaneous bleaching of the UPB and MPB states. After the signal build-up, the  
18 dynamics of the two polaritons look very different. In particular, the UPB undergoes a more  
19 rapid decay than the MPB, whose transient signal remains nearly constant over the first 500 fs.  
20 We ascribe such slow MPB dynamics to the balance between formation and decay mechanisms;

1 the formation is due to the relaxation from the UPB states, while the decay is due to relaxation  
2 to the LPB ground state. It is important to underline that our 2DES data do not allow to  
3 completely isolate the contribution of the exciton reservoir, since the linewidths of the excitons  
4 are broader with respect to the energy distance between the polariton states. For this reason, our  
5 results do not exclude a possible transfer from the UPB to the TDBC exciton reservoir, however  
6 they clearly show that the coupling between all the polariton states occurs on an ultrafast time  
7 scale.

8 Figure 3c plots cavity dynamics obtained following excitation at 1.96 eV (corresponding  
9 to the NK2707 exciton) and detection at energies corresponding to the cross peaks at 2.06 eV  
10 (MPB - orange) and 1.93 eV (LPB - green). We observe a nearly instantaneous rise in the  
11 signal, again confirming an immediate coupling with the cavity mode. The subsequent decay  
12 of the LPB is comparatively slower than that of the MPB; a result that likely signals a degree  
13 of exciton relaxation from the MPB to LPB states. Other possible relaxation pathways include  
14 scattering from MPB states to the exciton reservoir which then populate states in the LPB<sup>64-66</sup>.  
15 Therefore, the dynamics of LPB states may well be slower than the depopulation of the MPB  
16 because this likely involves partial filling of and then depopulation of the exciton reservoir.

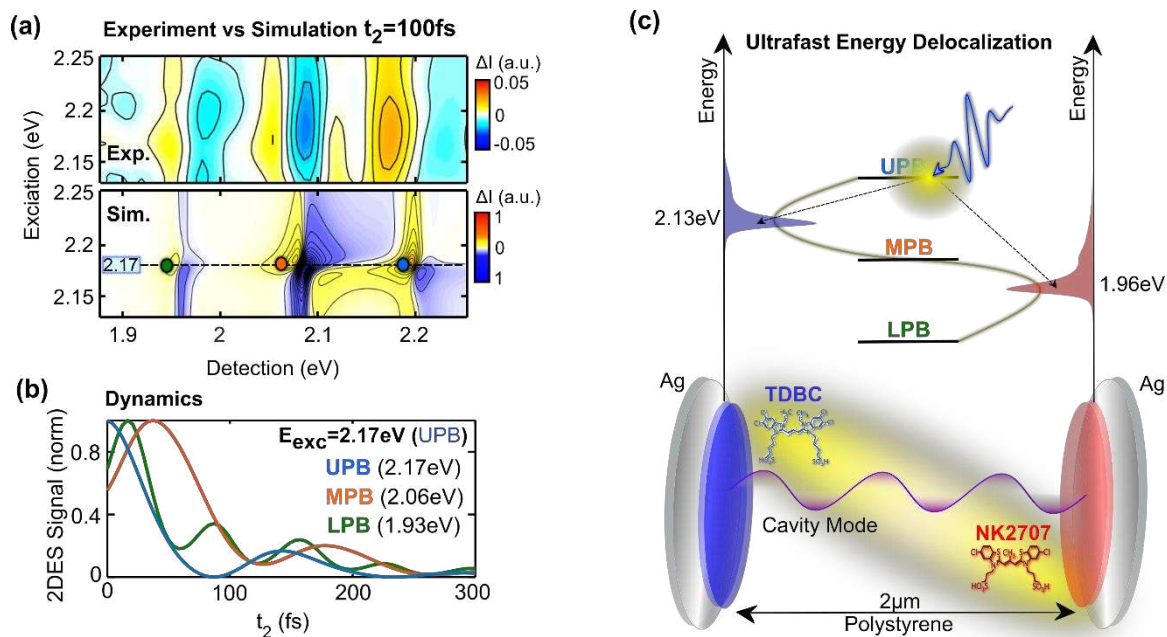
17 Finally, Figure 3d shows normalized cavity dynamics recorded following excitation of  
18 the UPB and detected at the diagonal peak at 2.17 eV (UPB, blue) and at the cross peaks 2.06  
19 eV (MPB, orange) and 1.93 eV (LPB, green). As expected, the signal from the UPB diagonal  
20 peak forms instantaneously; remarkably, the cross peaks detected at MPB and LPB also  
21 undergo a nearly instantaneous rise within the limit of the sub-20-fs experimental temporal  
22 resolution. Interestingly, the excitation of the UPB results in a detectable signal from the LPB,  
23 which is not visible following the excitation of the higher energy TDBC exciton.

24 Our measurements allow us to draw two main conclusions: i) coherent coupling occurs  
25 between the three polaritons states, however this is not observed following the direct excitation  
26 of the exciton reservoir and ii) the ultrafast formation of the transient signal detected at MPB  
27 and LPB energies following the excitation of the UPB suggests that the energy rapidly  
28 delocalizes throughout the entire cavity. This coupling drives energy delocalization between  
29 the different molecular species, even though they are physically separated by 2 $\mu$ m, a distance  
30 much greater than the Förster transfer radius. Note that this process still respects causality, and  
31 when using the term instantaneous we implicitly refer to timescales substantially longer than  
32 the inverse coupling frequencies between light and matter, which in our case are of the order of  
33 the experimental time resolution. To confirm our data, we performed additional measurements  
34 using broader pump and probe pulses, with spectrum spanning 1.77-2.25 eV which also excites

1 the  $\Gamma_3$  cavity mode. Again, we see a very similar phenomenology for the dynamics of the UPB,  
2 MPB and LPB (see Figure S3).

3 To gain further insight into this process, we have simulated the 2DES signal from the  
4 cavity using a fully coherent, broadband polaritonic model summarized in the Methods section  
5 and in the Supporting Information. The Methods section also discusses justifications and  
6 limitations of the theoretical model. Figure 4a (top panel) shows the experimental 2DES data  
7 at  $t_2 = 100$  fs limited to the excitation region from 2.13 eV to 2.25 eV to emphasize the cross  
8 peaks, with the bottom panel in Figure 4a being a theoretical simulation of the experimental  
9 data. While our coherent model is unable to provide quantitative predictions, it reproduces  
10 correctly the position of the polariton peaks and their derivative lineshape, validating our  
11 interpretation of instantaneous energy delocalization between the different exciton components  
12 driven by a single cavity mode. Here, we mark the peaks using coloured circles in panel a, and  
13 then plot their normalized simulated dynamics in Figure 4b. Specifically, the dynamics plotted  
14 are generated following simulated excitation at 2.17eV (UPB) and then detection at 2.17eV  
15 (blue), 2.06 eV (MPB, orange) and 1.93eV (LPB, green).

16 Comparing the dynamics calculated from the theoretical model excited at the UPB  
17 frequency to measured data in Figure 3d, we can see how the model reproduces some of the  
18 early-time features observed in the data, such as the slower rise-time of the signal detected at  
19 LPB and MPB frequencies with respect to the UPB. The model fails however to correctly  
20 reproduce the evolution of the signal at longer delay times due to its fully coherent nature,  
21 conflating populations and coherence lifetimes. This does not allow signal damping to be  
22 correctly described as it is visible by the much faster decays predicted by the theory as compared  
23 to measured data. We note that in the absence of dephasing, the theoretical model predicts  
24 coherent oscillations (see Figure 4b) due to beating between the different polariton modes, not  
25 sufficiently clear in the experimental observations, with these oscillations being akin to the Rabi  
26 oscillations observable in the time dynamics of strongly coupled systems.



1  
 2 **Figure 4.** Simulation and model: (a) Experimental data (top) and simulated signal (bottom)  
 3 purely absorptive 2DES map at  $t_2=100\text{fs}$  where the excitation axis is cut from 2.13eV to 2.25eV  
 4 and the detection axis is limited between 1.88eV and 2.25eV. (b) Simulated  $t_2$  traces of the  
 5 points indicated in the simulated 2DES map reported in part (a). Here such points are obtained  
 6 by exciting the UPB (2.17eV) and detecting the UPB (2.17eV, blue), MPB (2.06eV, orange)  
 7 and LPB (1.93eV, green). (c) Deactivation energy level scheme after the excitation of the UPB  
 8 state where dashed black arrows indicate an ultrafast delocalization of the energy among  
 9 exciton and polariton states. The yellow line in the energy level scheme (top) represents the  
 10 energy path that provides a connection between the TDBC and NK2707.

## 11 12 4. Conclusions

13 In summary, we exploited the combination of high temporal and spectral resolution of  
 14 2DES to reveal the mechanism of long-range ultrafast energy transfer between two dyes in a  
 15 strongly coupled organic microcavity. We study a multilayer comprised of two thin layers of  
 16 the J-aggregate dyes TDBC and NK2707 that were spatially separated by a  $2\mu\text{m}$  PS transparent  
 17 film. Our results show that this system behaves differently when located inside or outside a  
 18 microcavity. Specifically, when measured outside a cavity, we do not evidence any energy  
 19 transfer process between the two dyes, a result expected on the basis of the Förster transfer-  
 20 radius limit. 2DES measurements on the cavity indicate the presence of the polariton states due  
 21 to the strong coupling and the presence of cross peaks that are formed in a time scale comparable  
 22 with the temporal resolution of the experiment (20fs). Figure 4c schematically illustrates the  
 23 cavity system (bottom) and its energy levels (top). Here, we graphically represent the ultrafast

1 energy delocalization over the entire system obtained as a result of the excitation of the UPB  
2 state. Specifically, upon excitation of the UPB, energy is coherently delocalized throughout the  
3 entire cavity, providing a direct connection between the molecular excitons. Such a mechanism  
4 is supported by simulations of the 2DES data obtained using a model that considers interaction  
5 of the molecular excitons with a single cavity mode. Despite the fact that our model does not  
6 reproduce the amplitude of the various signals, it does allow us to predict the ultrafast formation  
7 of the cross peaks and their 2D lineshape. Our results should stimulate the design of innovative  
8 optoelectronic devices in which polariton states are exploited to drive efficient energy transfer  
9 among coupled chromophores.

## 11 **5. Experimental Section/Methods**

12 *Two-dimensional electronic spectroscopy (2DES)*: The experimental apparatus used in this  
13 work is described in detail elsewhere<sup>67</sup>. Briefly, the broadband laser pulses are generated by a  
14 non-collinear optical parametric amplifier (NOPA) pumped by an amplified Ti:Sapphire laser  
15 that generates 100-fs pulses at 1 kHz and 800 nm wavelength. The NOPA produces pulses with  
16 a 1.88-2.25 eV bandwidth, that are compressed to sub-20-fs duration using a pair of chirped  
17 mirrors. In this work, pump and probe laser pulses are frequency degenerate and we use a  
18 partially collinear pump-probe geometry in which the first two pulses are collinear and a third  
19 probe pulse, acts as local oscillator. The delay time  $t_1$  is controlled using a common-path  
20 birefringent interferometer, the Translating-Wedges-Based Identical pulses encoding System  
21 (TWINS) system<sup>68</sup>. In our experiment,  $t_1$  is scanned from -30fs to 250fs. The delay time  $t_2$  is  
22 controlled by a standard mechanical translation stage along the probe optical path and is  
23 scanned from -250 to 3000 fs. In all the experiments reported, the polarization between the  
24 pump and the probe beam was fixed at the magic angle ( $54.7^\circ$ ). The single-component  
25 molecular films and the multilayer film were measured in transmission and excited at a fluence  
26 of  $45 \mu\text{J}/\text{cm}^2$ . The organic microcavity however was measured in reflection at an incidence  
27 angle of  $10^\circ (\pm 5^\circ)$  and excited at a fluence of  $100\mu\text{J}/\text{cm}^2$ .

28  
29 *Control-film and Microcavity Fabrication*: J-aggregates NK2707 (supplied by Hayashibara  
30 Biochemical) and TDBC (supplied by FEW Chemicals GmbH) were dissolved at a  
31 concentration of 5% and 10% by weight in a deionized water / gelatine solution ( $20 \text{ mg mL}^{-1}$ ),  
32 respectively. J-aggregate / gelatine solutions were held at a temperature of  $65^\circ\text{C}$  before  $100 \mu\text{L}$   
33 of solution was used to spin-cast thin films. PS (supplied by Sigma-Aldrich) having a molecular  
34 weight of  $M_w \sim 350,000$  was dissolved in toluene at a concentration of  $100 \text{ mg mL}^{-1}$  and spin-

1 casted using 200  $\mu\text{L}$  of solution held at room temperature. Control over the thickness of the  
2 various thin layers was achieved by changing the rotation speed of the substrate during spin-  
3 casting, and was determined with a Bruker Dektak XT profilometer.

4  
5 An Ångström Engineering thermal evaporator was used to evaporate the microcavity Ag  
6 mirrors. The Ag deposition rate was maintained between 0.5 and 1  $\text{Å/s}^{-1}$  with the sample  
7 chamber being held at a base pressure of  $2 \times 10^{-6}$  mbar. The bottom and top mirrors had a  
8 thickness of 200 nm (fully reflective) and 34 nm (semi-transparent), respectively. The organic  
9 multilayers were fabricated by subsequently spin-casting the various J-aggregate / gelatine and  
10 PS layers, as described above.

11  
12 *Theoretical model:* General quantum theories of 2DES that are able to provide quantitative  
13 predictions need to consider both coherent and incoherent processes on the same footing.<sup>69</sup> This  
14 is due to the potential proximity of the timescales involved in the two kinds of processes in  
15 ultrafast optical experiments. Due to the inherent complexity of the many-body coupling  
16 between bright and dark states in polaritonic systems, alternative approaches are used to  
17 confirm qualitative interpretation of experimental data<sup>70</sup>. If delay times substantially longer than  
18 the cavity lifetime are considered, we can use a fully incoherent theory in which the oscillations  
19 of the short-lived polaritonic states interact nonlinearly with an incoherent reservoir of dark  
20 excitons. In our case a cavity lifetime of  $\sim 164$  fs is well resolved using our available temporal  
21 resolution. We thus used a complementary, fully coherent polaritonic model. In the same spirit  
22 we make a broadband approximation in which we neglect the temporal overlap between  
23 successive pulses. Note that for waiting times comparable or longer than the excitation  
24 lifetimes, the predictions of the fully coherent model regarding the absolute value of the signal  
25 intensity will necessarily degrade due to the absence of dark states. In other terms, in our theory  
26 populations and coherences have the same lifetime.

27  
28 As described in more details in the Supporting Information, we describe the pumped system  
29 using the non-Hermitian, non-linear Hamiltonian  $H = \sum_{\mathbf{q}} H_{\text{L}}(\mathbf{q}) + \sum_{\mathbf{q}, \mathbf{q}', \mathbf{q}''} H_{\text{NL}}(\mathbf{q}, \mathbf{q}', \mathbf{q}'')$ ,  
30 where the first term models the linear, lossy, and pumped system, and the second the cubic  
31 nonlinear interactions between cavity photons, TDBC excitons, and NK2707 excitons. We can  
32 solve  $H_{\text{L}}(\mathbf{q})$  by writing the time evolution of the photon and exciton fields under the effect of  
33 the external pump and of their mutual interactions and then inject these into  $H_{\text{NL}}(\mathbf{q}, \mathbf{q}', \mathbf{q}'')$  to  
34 calculate the induced third-order polarization. Such simulations are performed in the broadband



1 approximation, that is considering instantaneous pulses. This explains the non-zero value of the  
2 pumped mode obtained at  $t_2 = 0$ . The linear parameters required for the simulations are  
3 determined from the experimental steady state absorption spectrum of thin films containing  
4 each type of J-aggregated dye (see Figure 1) with the frequencies and linewidths of the different  
5 modes obtained by fitting the coupled resonances. The non-linear coefficients of the excitons  
6 have been calculated from the respective molecular densities using the Agranovich-Toshich  
7 transformation<sup>71</sup>, while the non-resonant non-linear coefficient of the photonic field,  
8 corresponding to the transparent polystyrene spacer-layer, has been taken from the literature<sup>72</sup>.  
9 The dynamical evolution of the system can then be written as a nonlinear wave equation  
10 coupling the cavity mode with the two excitonic resonances, and analytically solved in the  
11 broadband limit for the intensity of the photonic component which is proportional to the 2DES  
12 measured signal. More explicit calculations, as well the list of parameters used are given in the  
13 Supporting Information.

14

### 15 **Supporting Information**

16 Supporting Information is available from the Wiley Online Library or from the author.

17

### 18 **Acknowledgements**

19 S.D.L. acknowledges funding from the Leverhulme Trust (grant RPG-2022-037). D.G.L. and  
20 K.G. thank the U.K. EPSRC for funding via the Programme Grant ‘Hybrid Polaritonics’  
21 (EP/M025330/1). K.G. and A.O. acknowledge support from the University of Cyprus through  
22 the postdoctoral fellowship program ‘Onisilos’ M.M. acknowledges funding from the European  
23 Union (ERC-StG, ULYSSES, 101077181). Views and opinions expressed are however those  
24 of the author(s) only and do not necessarily reflect those of the European Union or the European  
25 Research Council. Neither the European Union nor the granting authority can be held  
26 responsible for them.

27

28 Received: ((will be filled in by the editorial staff))

29 Revised: ((will be filled in by the editorial staff))

30 Published online: ((will be filled in by the editorial staff))

31

32

33

34

1 **References**

- 2 [1] C. Weisbuch, M. Nishioka, A. Ishikawa, Y. Arakawa, *Phys. Rev. Lett.* **1992**, *69*, 3314–  
3 3317.
- 4 [2] A. V. Kavokin, J. J. Baumberg, G. Malpuech, F. P. Laussy, *Microcavities*, Second Edi  
5 Oxford Univ. Press, UK **2017**.
- 6 [3] P. G. Savvidis, J. J. Baumberg, R. M. Stevenson, M. S. Skolnick, D. M. Whittaker,  
7 and J. S. Roberts, *Phys. Rev. Lett.* **2000**, *84*, 1547–1550.
- 8 [4] J. Kasprzak, M. Richard, S. Kundermann, A. Baas, P. Jeambrun, J. M. J. Keeling, F.  
9 M. Marchetti, M. H. Szymańska, R. André, J. L. Staehli, V. Savona, P. B. Littlewood, B.  
10 Deveaud and Le Si Dang, *Nature* **2006**, *443*, 409–414.
- 11 [5] K. G. Lagoudakis, M. Wouters, M. Richard, A. Baas, I. Carusotto, R. André, Le Si  
12 Dang and B. Deveaud-Plédran, *Nat. Phys.* **2008**, *4*, 706–710.
- 13 [6] N. G. Berloff, M. Silva, K. Kalinin, A. Askitopoulos, J. D. Töpfer, P. Cilibrizzi, W.  
14 Langbein and P. G. Lagoudakis, *Nat. Mater.* **2017** *16*, 1120–1126.
- 15 [7] S. Klemmt, T. H. Harder, O. A. Egorov, K. Winkler, R. Ge, M. A. Bandres, M.  
16 Emmerling, L. Worschech, T. C. H. Liew, M. Segev, C. Schneider and S. Höfling, *Nature*  
17 **2018**, *562*, 552–556.
- 18 [8] D. G. Lidzey, D. D. C. Bradley, M. S. Skolnick, T. Virgili, S. Walker and D. M.  
19 Whittaker, *Lett. to Nat.* **1998** *395*, 53–55.
- 20 [9] Z. Jiang, A. Ren, Y. Yan, J. Yao, Y. S. Zhao, *Adv. Mater.* **2022**, *34*, 2106095.
- 21 [10] J. D. Plumhof, T. Stoeferle, L. Mai, U. Scherf, R. F. Mahrt, *Nat. Mater.* **2014**, *13*,  
22 247–252.
- 23 [11] K. S. Daskalakis, S. A. Maier, R. Murray, S. Kéna-cohen, *Nat. Mater.* **2014**, *13*, 271–  
24 278.
- 25 [12] G. Lerario, D. Ballarini, A. Fieramosca, A. Cannavale, A. Genco, F. Mangione, S.  
26 Gambino, L. Dominici, M. De Giorgi, G. Gigli and D. *Light Sci. Appl.* **2017**, *6*, e16212.
- 27 [13] R. Jayaprakash, C. E. Whittaker, K. Georgiou, O. S. Game, K. E. McGhee, D. M.  
28 Coles, and D. G. Lidzey, *ACS Photonics* **2020**, *7*, 2273–2281.
- 29 [14] C. P. Dietrich, A. Steude, L. Tropsch, M. Schubert, N. M. Kronenberg, K. Ostermann, S.  
30 Höfling, and M. C. Gather, *Sci. Adv.* **2016**, *2*, e1600666.
- 31 [15] T. Cookson, K. Georgiou, A. Zasedatelev, R. T. Grant, T. Virgili, M. Cavazzini, F.  
32 Galeotti, C. Clark, N. G. Berloff, D. G. Lidzey, P. G. Lagoudakis, *Adv. Opt. Mater.* **2017**, *5*,  
33 1700203.

- 1 [16] A. Putintsev, A. Zasedatelev, K. E. McGhee, T. Cookson, K. Georgiou, D. Sannikov,  
2 D. G. Lidzey, P. G. Lagoudakis, *Appl. Phys. Lett.* **2020**, *117*, 123302.
- 3 [17] T. Yagarof, D. Sannikov, A. Zasedatelev, K. Georgiou, A. Baranikov, O. Kyriienko, I.  
4 Shelykh, L. Gai, Z. Shen, D. Lidzey, P. Lagoudakis, *Commun. Phys.* **2020**, *3*, 1–10.
- 5 [18] A. V. Zasedatelev, A. V. Baranikov, D. Urbonas, F. Scafirimuto, U. Scherf, T.  
6 Stöferle, R. F. Mahrt and P. G. Lagoudakis, *Nat. Photonics* **2019**, *13*, 378–383.
- 7 [19] J. Tang, J. Zhang, Y. Lv, H. Wang, F. F. Xu, C. Zhang, L. Sun, J. Yao, Y. S. Zhao,  
8 *Nat. Commun.* **2021**, *12*, 3265.
- 9 [20] W. Ahn, F. Herrera, B. Simpkins, *Modification of Urethane Addition Reaction via*  
10 *Vibrational Strong Coupling*. ChemRxiv. Cambridge: Cambridge Open Engage, **2022**
- 11 [21] F. Herrera, J. Owirutsky, *J. Chem. Phys.* **2020**, *152*, 100902.
- 12 [22] D. Polak, R. Jayaprakash, T. P. Lyons, L. Á. Martínez-Martínez, A. Leventis, K. J.  
13 Fallon, H. Coulthard, D. G. Bossanyi ORCID logoa, Kyriacos Georgiou a, Anthony J. Petty,  
14 II a, John Anthony, H. Bronstein, J. Yuen-Zhou, A. I. Tartakovskii, J. Clark and A. J. Musser,  
15 *Chem. Sci.* **2020**, *11*, 343–354.
- 16 [23] L. A. Martínez-Martínez, M. Du, R. F. Ribeiro, S. Kéna-Cohen, J. Yuen-Zhou, *J.*  
17 *Phys. Chem. Lett.* **2018**, *9*, 1951–1957.
- 18 [24] E. Eizner, L. A. Martínez-Martínez, J. Yuen-Zhou, S. Kéna-Cohen, *Sci. Adv.* **2019**, *5*,  
19 1–9.
- 20 [25] Y. Yu, S. Mallick, M. Wang, K. Börjesson, *Nat. Commun.* **2021**, *12*, 2–9.
- 21 [26] R. Pandya, A. Ashoka, K. Georgiou, J. Sung, R. Jayaprakash, S. Renken, L. Gai, Z.  
22 Shen, A. Rao, A. J. Musser, *Adv. Sci.* **2022**, *9*, 2105569.
- 23 [27] A. Thomas, L. Lethuillier-Karl, K. Nagarajan, R. M. A. Vergauwe, J. George, T.  
24 Chervy, A. Shalabney, E. Deveaux, C. Genet, J. Moran and T. W. Ebbesen, *Science* **2019**,  
25 *363*, 615–619.
- 26 [28] J. Galego, F. J. Garcia-Vidal, J. Feist, *Phys. Rev. X* **2015**, *5*, 041022.
- 27 [29] S. Kéna-Cohen, J. Yuen-Zhou, *ACS Cent. Sci.* **2019**, *5*, 386–388 (2019).
- 28 [30] M. Du, L. A. Martinez-Martinez, R. F. Ribeiro, Z. Hu, V. M. Menon, J. Yuen-Zhou,  
29 *Chem. Sci.* **2019**, *10*, 10821.
- 30 [31] D. M. Coles, N. Somaschi, P. Michetti, C. Clark, P. G. Lagoudakis, P. G. Savvidis and  
31 D. G. Lidzey, *Nat. Mater.* **2014**, *13*, 712–719.
- 32 [32] X. Zhong, T. Chervy, S. Wang, J. George, A. Thomas, J. A. Hutchison, E. Devaux, C.  
33 Genet, T. W. Ebbesen, *Angew. Chem.* **2016**, *55*, 6202–6206.

- 1 [33] X. Zhong, T. Chervy, L. Zhang, A. Thomas, J. George, C. Genet, J. A. Hutchison, T.  
2 W. Ebbesen, *Angew. Chem.* **2017**, *56*, 9034–9038 (2017).
- 3 [34] K. Georgiou, R. Jayaprakash, A. Othonos, D. G. Lidzey, *Angew. Chem.* **2021**, *133*,  
4 16797-16803.
- 5 [35] C. Sánchez Muñoz, F. Nori, S. De Liberato, *Nat. Commun.* **2018**, *9*, 1924.
- 6 [36] T. Virgili, D. Coles, A. M. Adawi, C. Clark, P. Michetti, S. K. Rajendran, D. Brida, D.  
7 Polli, G. Cerullo, and D. G. Lidzey, *Phys. Rev. B* **2011**, *83*, 245309.
- 8 [37] S. Takahashi, K. Watanabe, Y. Matsumoto, *J. Chem. Phys.* **2019**, *151*.
- 9 [38] T. Schwartz, J. A. Hutchison, J. Léonard, C. Genet, S. Haacke, T. W. Ebbesen, *Chem.*  
10 *Phys. Chem.* **2013**, *14*, 125–131.
- 11 [39] C. A. DelPo, B. Kudisch, K. H. Park, S.-U.-Z. Khan, F. Fassioli, D. Fausti, B. P. Rand,  
12 and G. D. Scholes, *J. Phys. Chem. Lett.* **2020**, *11*, 2667–2674.
- 13 [40] A. G. Avramenko, A. S. Rury, *J. Phys. Chem. Lett.* **2020**, *11*, 1013–1021.
- 14 [41] G. G. Rozenman, K. Akulov, A. Golombek, T. Schwartz, *ACS Photonics* **2018**, *5*,  
15 105–110.
- 16 [42] L. Mewes, M. Wang, R. A. Ingle, K. Börjesson, M. Chergui, *Commun. Phys.* **2020**, *3*,  
17 157.
- 18 [43] J. M. Lüttgens, Z. Kuang, N. F. Zorn, T. Buckup, J. Zaumseil, *ACS Photonics* **2022**, *9*,  
19 5, 1567–1576.
- 20 [44] S. Renken, R. Pandya, K. Georgiou, R. Jayaprakash, L. Gai, Z. Shen, D. G. Lidzey,  
21 A. Rao, A. J. Musser, *J. Chem. Phys.* **2021**, *155*, 154701.
- 22 [45] J. Keeling, S. Kéna-Cohen, *Annu. Rev. Phys. Chem.* **2020**, *71*, 435–459.
- 23 [46] V. M. Agranovich, M. Litinskaya, D. G. Lidzey, *Phys. Rev. B* **2003**, *67*, 085311.
- 24 [47] M. Litinskaya, P. Reineker, V. M. Agranovich, *J. Lumin.* **2004**, *110*, 364–372.
- 25 [48] E. Michail, K. Rashidi, B. Liu, G. He, V. M. Menon, M. Y. Sfeir, *Nano Lett.* **2024**, *24*,  
26 557–565.
- 27 [49] S. Mukamel, *Annu. Rev. Phys. Chem.* **2000**, *51*, 691–729.
- 28 [50] D. M. Jonas, *Annu. Rev. Phys. Chem.* **2003**, *54*, 425–463.
- 29 [51] B. Xiang, R. F. Ribeiro, M. Du, L. Chen, Z. Yang, J. Wang, J. Yuen-Zhou, W. Xiong,  
30 *Science*, **2020**, *368*, 665-667.
- 31 [52] R. T. Allen, A. Dhavamani, M. Son, S. Kéna-Cohen, M. T. Zanni, M. S. Arnold, *J. Phys.*  
32 *Chem. C*, **2022**, *126*, 8417–8424.
- 33 [53] M. Son, Z. T. Armstrong, R. T. Allen, A. Dhavamani, M. S. Arnold, M. T. Zanni, *Nat.*  
34 *Commun.*, **2022**, *13*, 7305.

- 1 [54] G. G. Paschos, N. Somaschi, S. I. Tsintzos, D. Coles, J. L. Bricks, Z. Hatzopoulos, D.  
2 G. Lidzey, P. G. Lagoudakis and P. G. Savvidis, *Sci. Rep.* **2017**, *7*, 11377.
- 3 [55] R. Jayaprakash, K. Georgiou, H. Coulthard, A. Askitopoulos, S. K. Rajendran, D. M.  
4 Coles, A. J. Musser, J. Clark, I. D. W. Samuel, G. A. Turnbull, P. G. Lagoudakis and D. G.  
5 Lidzey, *Light Sci. Appl.* **2019**, *8*, 81.
- 6 [56] I. Stiopkin, T. Brixner, M. Yang, G. R. Fleming, *J. Phys. Chem. B* **2006**, *110*,  
7 20032–20037.
- 8 [57] L. Luer, S. K. Rajendran, T. Stoll, L. Ganzer, J. Rehault, D. M. Coles, D. Lidzey, T.  
9 Virgili, G. Cerullo, *J. Phys. Chem. Lett.* **2017**, *8*, 547–552.
- 10 [58] R. Moca, S. R. Meech, I. A. Heisler. *J. Phys. Chem. B.* **2015**, *119*, 8623–8630.
- 11 [59] S. Richter, T. Michalsky, L. Fricke, C. Sturm, H. Franke, M. Grundmann, and R.  
12 Schmidt-Grund, *Appl. Phys. Lett.* **2015**, *107*, 231104.
- 13 [60] M. Balasubrahmaniyam, C. Genet, and T. Schwartz, *Phys. Rev. B* **2021**, *103*,  
14 L241407.
- 15 [61] K. Georgiou, K.E. McGhee, R. Jayaprakash, and D.G. Lidzey, *J. Chem. Phys.* **2021**,  
16 *154*, 124309.
- 17 [62] M. Godsi, A. Golombek, M. Balasubrahmaniyam, and T. Schwartz, *J. Chem. Phys.*  
18 **2023**, *159*, 134307.
- 19 [63] T. Virgili, D. G. Lidzey, D. D. C. Bradley, G. Cerullo, S. Stagira, and S. De Silvestri,  
20 *Appl. Phys. Lett.* **1999**, *74*, 2767.
- 21 [64] D.M. Coles, P. Michetti, C. Clark, W.C. Tsoi, A.M. Adawi, J.S. Kim, and D.G. Lidzey,  
22 *Adv. Funct. Mater.* **2011** *21*, 3691-3696.
- 23 [65] R.T. Grant, P. Michetti, A.J. Musser, P. Gregoire, T. Virgili, E. Vella, M. Cavazzini, K.  
24 Georgiou, F. Galeotti, C. Clark, J. Clark, C. Silva, and D.G. Lidzey, *Adv. Opt. Mater.* **2016** *4*,  
25 1615-1623.
- 26 [66] K. Georgiou, R. Jayaprakash, A. Askitopoulos, D.M. Coles, P.G. Lagoudakis, and D.G.  
27 Lidzey, *ACS Photonics* **2018** *5*, 4343–4351.
- 28 [64] J. Rehault; M. Maiuri; A. Oriana; G. Cerullo, *Rev. Sci. Instrum.* **2014**, *85*,1–10.
- 29 [65] D. Brida, C. Manzoni; G. Cerullo, *Optics Letters* **2012**, *37*, 3027–3029.
- 30 [66] V. Butkus, D. Abramavicius, A. Gelzinis, L. Valkunas, *Lithuanian Journal of Physics*  
31 **2010**, *50*, 267-303.
- 32 [67] B. Xiang, R. F. Ribeiro, A. D. Dunkelberger, J. Wang, Y. Li, B. S. Simpkins, J. C.  
33 Owrutsky, J. Yuen-Zhou, W. Xiong, *Proc. Natl. Acad. Sci.* **2018**, *115*, 4845-4850.
- 34 [68] V.M.Agranovich and B.S.Toshich, *Sov. Phys. JETP* **1968**, *26*, 104-112.

1 [69] Y. Liu, F. Qin, Z.-Y. Wei, Q.-B. Meng, D.-Z. Zhang, and Z.-Y. Li, *Appl. Phys. Lett.*  
2 **2009**, *95*, 131116.

3  
4

### Table of contents:

Our work demonstrates how the strong light-matter coupling regime in an organic microcavity can be used to engineer energetic interactions between molecular films separated by several microns. The quasi-instantaneous long-range electronic delocalization is driven by hybrid polaritonic states, as supported by a theoretical model. Our finding opens new perspectives on remote photo/induced energy transport useful in advanced optoelectronic devices.

M. Russo, K. Georgiou, A. Genco, S. De Liberato, G. Cerullo, D. G. Lidzey, A. Othonos, M. Maiuri\*, T. Virgili\*

Direct Evidence of Ultrafast Energy Delocalization Between Optically Hybridized J-Aggregates in a Strongly Coupled Microcavity

ToC figure

